coatings

MDPI

Article

Fabrication of Composites of Sodium Alginate with Guar Gum and Iron Coated Activated Alumina for the Purification of Water from Direct Blue 86

Samia Kanwal [1], Ali Irfan [2], Sami A. Al-Hussain [3], Gulnaz Sharif [4], Amina Mumtaz [1], Fozia Batool [1,*] and Magdi E. A. Zaki [3,*]

[1] Institute of Chemistry, University of Sargodha, Sargodha 40100, Pakistan
[2] Department of Chemistry, Government College, University Faisalabad, Faisalabad 38000, Pakistan
[3] Department of Chemistry, College of Science, Imam Mohammad Ibn Saud Islamic University (IMSIU), Riyadh 13623, Saudi Arabia
[4] Government Postgraduate College for Women Mandi Bahauddin 50400, Pakistan
* Correspondence: fozia.batool@uos.edu.pk (F.B.); mezaki@imamu.edu.sa (M.E.A.Z.); Tel.: +92-34-4747-4109 (F.B.)

Abstract: This study aims to purify water from hazardous dyes and for this purpose, a novel adsorbent is developed that was synthesized by using sodium alginate, guar gum and iron coated activated alumina (SA@GG@ICAA Composites) with the Ion Gelation Method. The novel composites were characterized by using SEM, XRD, DSC, FTIR, BET, EDX, zeta potential and zeta sizer. These novel composites were used for the removal of Direct Blue 86 (DB86). The surface area of the adsorbent was found to be 5.606 m^2/g. Zeta size and zeta potential was found to be 169.9 nm and −47.7 mV, respectively. Optimized parameters were achieved for best adsorption of the selected dye. For DB86, the removal efficiency was found to be 97% at 40 ppm (dye concentration), 150 min (contact time), 3 (pH) and 150 mg (adsorbent concentration) at λmax of 620 nm. Linear and non-linear forms of adsorption isotherms are applied on the experimental data to check the adsorption methodology and its chemistry. The non-linear form of the Freundlich isotherm was found to be best fitted for the current work (0.942) as compared with the linear form (0.76). The first order kinetics model and second order kinetics model are applied in both linear and non-linear forms, and results with a high R^2 value were obtained for the non-linear form of pseudo-first order kinetics. The adsorption mechanism was found to be electrostatic based on the interaction of the adsorbent and dye. Synthesized adsorbent can be successfully applied for the removal of DB86 dye from waste water.

Keywords: fabrication; composites; direct blue 86; water purification; dye removal; water pollution

check for updates

Citation: Kanwal, S.; Irfan, A.; Al-Hussain, S.A.; Sharif, G.; Mumtaz, A.; Batool, F.; Zaki, M.E.A. Fabrication of Composites of Sodium Alginate with Guar Gum and Iron Coated Activated Alumina for the Purification of Water from Direct Blue 86. *Coatings* **2023**, *13*, 103. https://doi.org/10.3390/coatings13010103

Academic Editors: Monica Trif, Alexandru Rusu and Sneh Punia Bangar

Received: 25 November 2022
Revised: 12 December 2022
Accepted: 15 December 2022
Published: 5 January 2023

Copyright: © 2023 by the authors. Licensee MDPI, Basel, Switzerland. This article is an open access article distributed under the terms and conditions of the Creative Commons Attribution (CC BY) license (https://creativecommons.org/licenses/by/4.0/).

1. Introduction

The anthropological activity which includes industrialization plays an adverse role in the pollution and destruction of the environment. It has an immensely hazardous impact on the health of the people [1,2]. Water is an essential factor for the sustenance of life and its significance cannot be overlooked. Whether it is used in excess amounts in industries or for drinking purposes, it's worth remains immeasurable. Hence, it is necessary not to allow the attenuation of water, which is either through contamination or its impetuous use, and can pose serious health problems, threats and challenges to human beings [3,4].

The textile industry is the one of the most ancient and highly advanced amongst the industrial sectors of the world economy which fulfils rising everyday human demands for textile products. The number of textile mills and the waste water they produce has been increasing correspondingly, which is seriously contributing to global pollution. Textile industry is using almost 2/3 of dye stuff for the dying purpose. About 10 to 15 percent of the

dyes used during the dyeing process are discharged into waste water. It is acknowledged as a primary contributor to environmental pollution. Numerous chemicals used in the textile industry are harmful to the environment and human health. Dyes are regarded as major contaminants of waste water from the textile industry. Water pollution that is linked to the textile industry causes environmental problems worldwide. Discharge of toxic chemicals and untreated waste into water bodies is causing water pollution. It also prevents light from passing through water bodies, which causes harm to the aquatic ecosystem [5,6].

Dyes are extremely poisonous and have a significant potential to cause eutrophication. Direct Blue 86 belongs to the Phthalocyanine class and is basically a direct, or acid/anionic dye. The toxicity of Direct Blue 86 was determined by using fresh water fish *Gambusiaaffinis* and an aquatic freshwater plant *Lemnaaequinoctialis*. The result shows that Direct Blue 86 is toxic to both aquatic plants and fish. The mortality test proves that Direct Blue 86 is toxic to zooplankton and thereby, to the environment [7].

Based on injurious health and environmental effects of Direct Blue 86 it is necessary to remove this dye from waste water of industries before disposal. In this regard several methods are employed, but the high cost of these techniques makes them unfavorable for the purpose. A cost effective and efficient way is the method of adsorption of dye on different materials [8]. Adsorbents are the solid substances which are employed for the elimination of hazardous, toxic and poisonous contaminants or pollutants from the waste water of industries. The characteristics for an effective adsorbent material include adequate pore size, good mechanical characteristics, widely attainable, high surface area and the presence of suitable functional groups such as amine groups, hydroxyl groups, and many others. A natural polysaccharide, sodium alginate is derived from brown algae and it fulfills all these requirements. This polymer has some excellent properties such as renewability, biocompatibility and biodegradability. Composites with other substances, surface grafting and cross-linking are the modification methodologies employed on sodium alginate-based adsorbents. It also shows dielectric properties when its composites are prepared with titanium dioxide [9]. Zou et al. (2019) prepared an innovative adsorbent by the emulsion polymerization of sodium alginate with acrylamide and polyacrylamide/sodium alginate, which was employed to remove methylene blue dye from waste water. Verma et al. (2020) prepared a sodium alginate/graphite-based hybrid hydrogel as an efficient and potential adsorbent for the removal of Malachite Green dye from waste water. Zhao et al. (2021) prepared fibrous chitosan/sodium alginate composite foams for the removal of methylene blue and Acid Black-172 [10,11].

The seeds of the Leguminosae family plant *Cyamopsis tetragonoloba* are used to make guar gum. Guar gum is a natural and cationic (positively charged) polysaccharide. Guar gum and its derivatives can be used as an effective adsorbent. Naserzade et al. (2022) prepared polyacrylic acid/guar gum/titanium dioxide hydrogels, a guar gum-based adsorbent for the removal of methylene blue dye from waste water.

Iron coated activated alumina is used as an effective adsorbent for the removal of dyes. Mahapatra et al. (2013) prepared an adsorbent by mixing iron oxide and alumina (Fe_2O_3/Al_2O_3) through the hydrothermal method for the removal of Congo red dye from waste water. Keeping in view the effectiveness of all these adsorbents, it is important to enhance their adsorption potential by synthesizing composites based on their derivatives.

In the present study, novel composites of sodium alginate, guar gum and iron coated activated alumina (SA@GG@ICAA) were prepared for the removal of DB86 dye from wastewater with a high removal efficiency of 97 percent. The synthesized adsorbent showed exceptional removal efficiency in comparison to reported adsorbents. Iron coated activated alumina was cross linked with guar gum and sodium alginate by using calcium chloride for synthesis of these novel composites. Moreover, the effect of various parameters such as initial concentration of dye, pH, contact time and adsorbent concentration on dye adsorption behavior of the cross linked composites was discussed. Adsorption Isotherms and reaction kinetics were applied for the study of the adsorption behavior of the dye on

the novel adsorbent. Synthetic composites were characterized in terms of FTIR, SEM, XRD and zeta sizer. Synthetic composites are found stable and efficient for the removal of DB86 from aqueous media.

2. Materials and Methods

2.1. Materials

Sodium hydroxide (98%–100%), acetic acid (99%), methanol (99.5%), calcium chloride (96%), sodium alginate and guar gum were purchased from Sigma Aldrich and of analytical grade. Iron coated granular activated alumina was purchased from Axens Group of Technologies, Made in Brockville, Canada and of commercial grade. Direct Blue 86/Direct Fast Turquoise Blue GL was purchased from the BDH Laboratories, Poole, UK and of analytical grade. Distilled water was obtained from the Khushab Water Plant, University of Sargodha, Sargodha, Pakistan and of analytical grade.

2.2. Adsorbent Preparation

The ion gelation method is used for the preparation of the adsorbent. A total of 10 g of sodium alginate and 1 g of guar gum is taken and homogenously dissolved in water and stirred for 4–5 h. Next, 10 g of iron coated activated alumina powder is mixed in water and stirred for 4–5 h in a separate beaker. The mixture of sodium alginate and guar gum is added to the solution of iron coated activated alumina and mixed well by stirring. In this way, iron coated activated alumina is impregnated in the mixture. Hence, the mixture of impregnated iron coated activated alumina in sodium alginate and guar gum is prepared [12].

For the preparation of novel composites, a cross-linker is used and, in this case, calcium chloride is used as the cross-linker. A 3% solution of calcium chloride is prepared (3 g of calcium chloride is dissolved in 100 mL water). A 5cc syringe is filled with mixture of impregnated iron coated activated alumina in sodium alginate and guar gum. This mixture is then added dropwise gradually in the 3% solution of calcium chloride using the 5cc syringe attached with an IV-Cannula gauge-24. The round spherical composites are formed in the calcium chloride solution and the composites are suspended in the solution for 48 h. After 48 h, the calcium chloride solution is filtered and the composites remain on the filter paper. The composites are rinsed with distilled water to remove the calcium, after the complete removal of calcium chloride, the composites are dried. The dried composites are then ground into a fine powder and passed through very fine sieves to obtain the fine composites. They are ground into fine particles to increase the surface area of the composites for better adsorption of dyes. Schematic diagram for the components is given in Figure 1.

2.3. Characterization of Composites

The characterization of the adsorbent is investigated by many analytical techniques, which are as follows: FTIR (Model No: Shimadzu FTIR 8400S, Kyoto, Japan), SEM (FEI Nova, Nano-SEM 450, Lausanne, Switzerland), zeta Potential and zeta Sizer (Model No: Joel JSM-IT100, Peabody, MA, USA), BET (Quantachrome instruments, Model No. Autosorb IQ-C-MP-AG (2 Stat.) Viton ID 195400, Boynton Beach, FL, USA), XRD (JEOL X-Ray Diffractometer system JDX-3532, Peabody, MA, USA), EDX (FEI Nova, Nano-SEM 450, Lausanne, Switzerland), DSC (Model No: Mettler Toledo Star SW 9.01, Greifensee, Switzerland) and UV/Visible Spectrophotometry (Peak Instruments, Houston, TX, USA, Model No. C-7200). These techniques play a very important role in the characterization of the adsorbent. It is a very crucial step for determining the characteristics of the adsorbent to achieve the desired results.

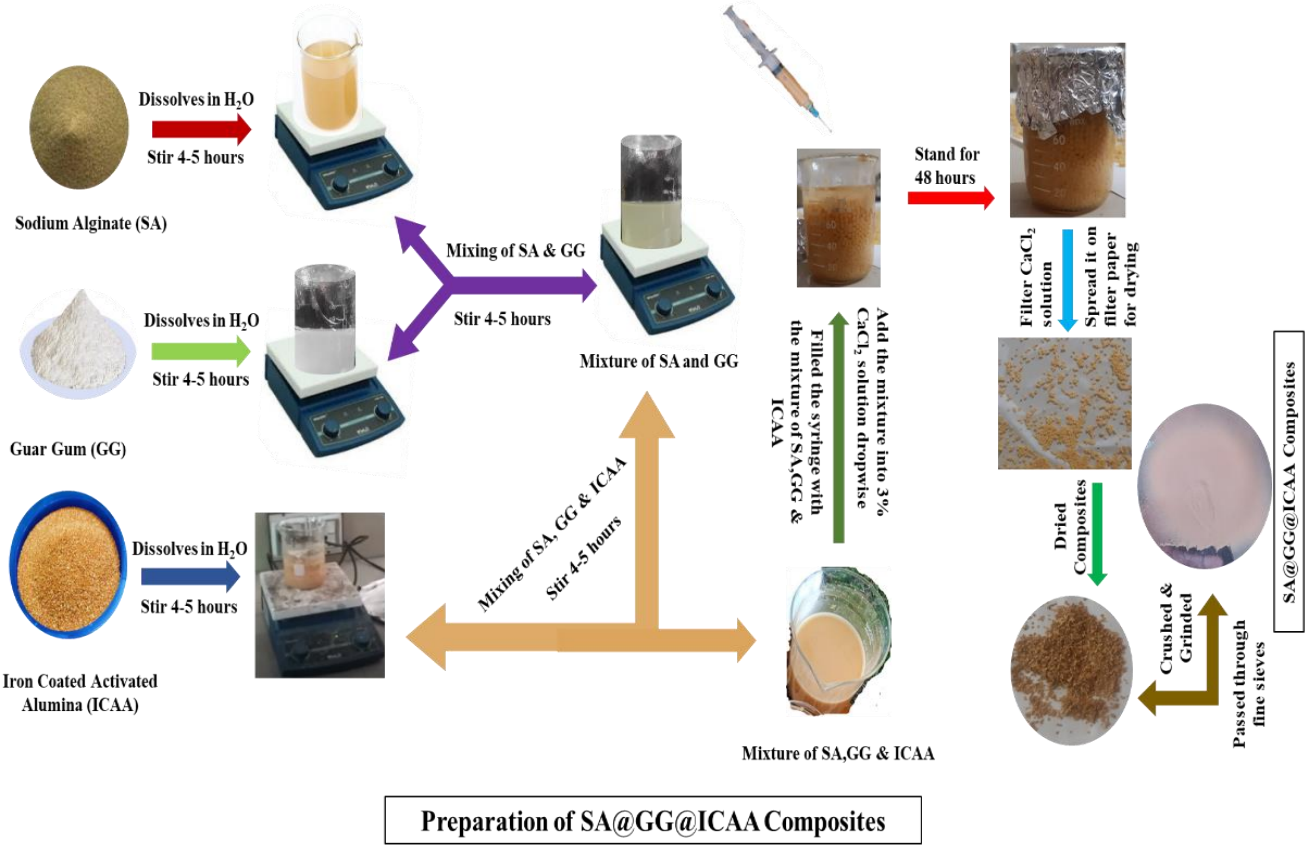


Figure 1. Synthetic Scheme of Composites.

2.4. Batch Experiment and Parameters Optimization

The batch experiment was designed to assess the adsorption capacity of the above prepared adsorbent. For this purpose, parameters of the optimization technique were applied and the following factors were varied to optimize the conditions. The batch experiments were performed on the following dye: (Direct Blue 86/Direct Fast Turquoise Blue GL Dye).

Initial concentration of dye has important effect on the adsorption phenomenon, as by varying the number of dye molecules the adsorption potential of the composites also changes. Thus, dye concentration was varied from 20 to 200 ppm. For this purpose, the experiment was performed on 20 ppm, 40 ppm, 60 ppm, 80 ppm, 100 ppm, 120 ppm, 140 ppm, 160 ppm, 180 ppm and 200 ppm dye concentration with the same amount of composites and the same contact time. The adsorbed amount of dye was determined using a UV/Visible spectrophotometer at 620 nm.

Contact time has significant role in the adsorption phenomenon so in current study adsorption was performed at six different time intervals ranging from 30 to 180 min. The adsorption phenomenon is also dependent on the pH of the solution from which dyes are removed. In order to monitor this factor, adsorption was performed at three different pH levels that included 3, 7 and 12.

2.5. Adsorption Isotherms and Kinetics

Adsorption isotherms are useful for describing the adsorption phenomenon on the surface of adsorbent. For the current study Freundlich, Langmuir, Dubinin–Radushkevich (R–D), Elovich and Temkin adsorption isotherms were applied on experimental data. Similarly, first order kinetic studies were also performed, followed by pseudo-first and -second order kinetic application on the data.

3. Results and Discussion

The present work was focused on green chemistry and for this purpose, non-toxic, environmentally friendly and cost-effective polymers, such as sodium alginate and guar gum were used for the preparation of the novel composites followed by the impregnation of iron coated activated alumina. Impregnation of the modified alumina makes the composites environmentally friendly, non-toxic and a green adsorbent for the removal of dyes for the purification of industrial waste water.

3.1. Adsorbent Morphology and Structure

It was studied using FTIR, SEM, EDX, XRD, DSC, BET, Zeta Sizer and Zeta Potential.

XRD spectrum is plotted between intensity on the y-axis and 2θ on the x-axis. In this spectrum, the value of 2θ ranges from 4.5–81°. The XRD of pure composites of SA@GG@ICAA were analysed as shown in Figure 2. The peaks that appeared at 7.201°, 13.277°, 20.965° and 31.319° are in good agreement with the reported values of sodium alginate, which indicates the presence of sodium alginate. The peaks that appeared at 17.307° and 20.221° indicate the presence of guar gum. Reported data showed the amorphous structure of guar gum [13]. The peaks that appeared at 25.057°, 32.187°, 35.039°, 37.333°, 38.387°, 43.471°, 45.579°, 67.093°, 68.093° and 78.501° indicate the presence of activated alumina and peaks that appeared at 30.575° and 36.527° indicate the presence of iron coated activated alumina [14]. Although sodium alginate in its pure form shows a semi-crystalline spectrum, in prepared composites it loses this behaviour and new synthetic composites are found amorphous in nature. A similar change in crystallinity is reported in previous data as well [15,16].

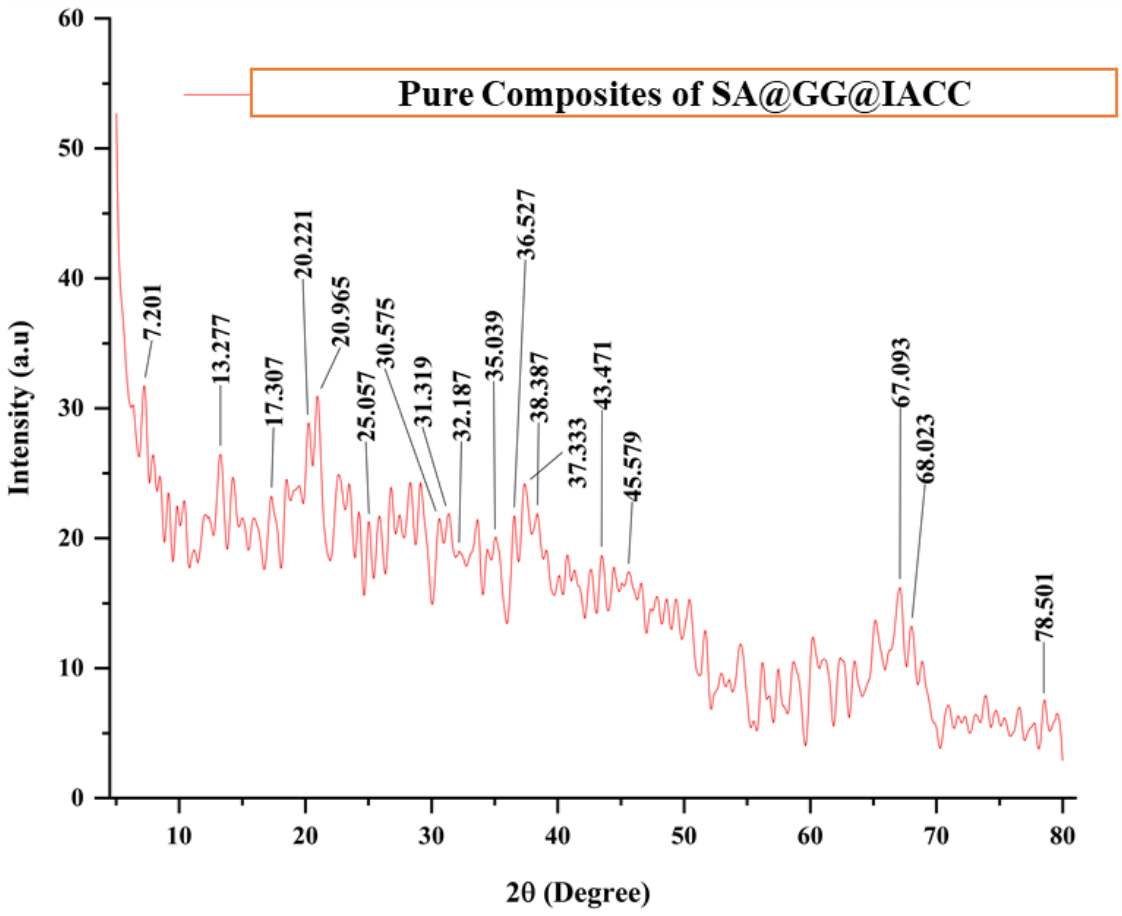


Figure 2. XRD Spectrum of SA@GG@ICAA Composites (Before Adsorption).

SEM of SA@GG@IACC Composites (before adsorption) was performed. Micrographs are taken at different magnifications and resolutions. The surface of the adsorbent appeared to be rough. The red arrows showed the presence of iron coated activated alumina entrapped in sodium alginate and guar gum composites. Small sized composites and some large sized particles are present. Agglomeration of some composites occurred. Similarly large number of hollow cavities and pores are available for adsorption. These cavities vary in size. These cavities may serve as an active site for adsorbate molecules. A large number of entrapped iron coated activated alumina particles are observed. The results which are obtained by SEM are in good agreement with the reported data (Figure 3).

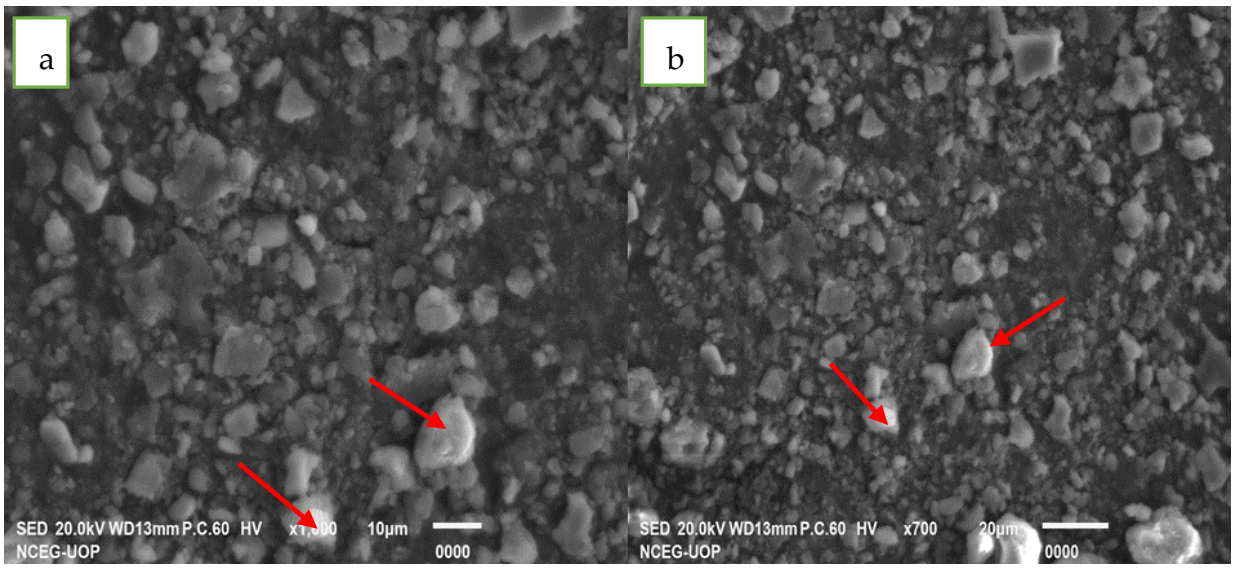


Figure 3. SEM of SA@GG@IACC Composites (**a**) Magnification = ×1400, Resolution = 10 µm, (**b**) Magnification = ×2700, Resolution = 5 µm.

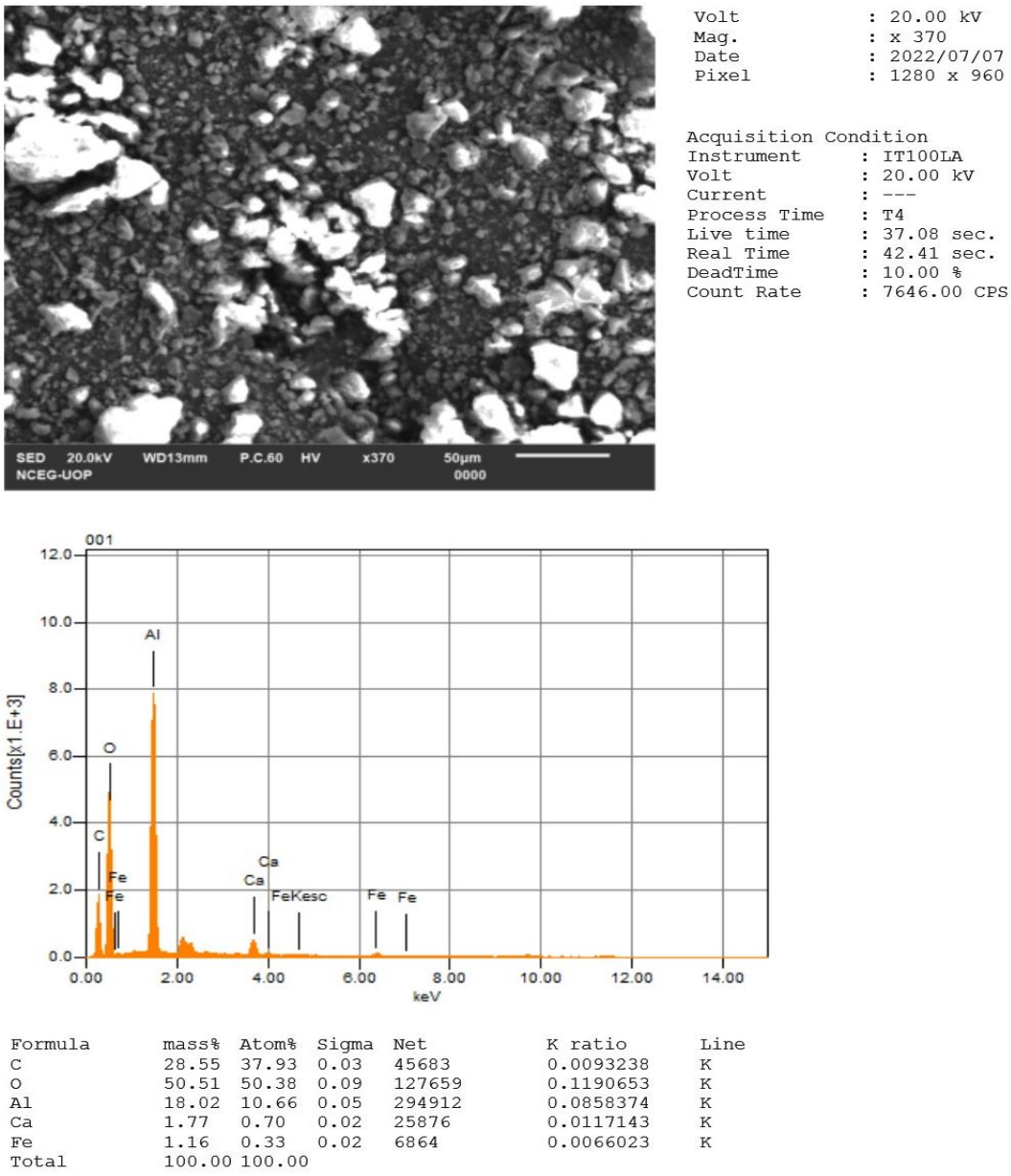
EDX of SA@GG@IACC Composites (before adsorption) was performed as given in Figure 4. The result showed the presence of carbon, oxygen, iron, aluminum and calcium. The mass percentage of C, O, Fe, Al and Ca was found to be 28.55, 50.51, 1.16, 18.02 and 1.77% respectively. The atom percentage of C, O, Fe, Al and Ca was found to be 37.93, 50.38, 0.33, 10.66 and 0.70 respectively. Some trace of calcium is found in the composites because calcium chloride was used as a cross-linker in their formation. Fe and Al are found in the composites which indicated the presence of iron coated activated alumina.

DSC of SA@GG@ICAA Composites (before adsorption) was performed as shown in Figure 5 and four peaks were obtained. Two peaks were endothermic and two peaks were exothermic. In the first run, endothermic peak 1 showed at 107.53 °C and exothermic peak 1 appeared at 241 °C. During cooling, exothermic peak 2 appeared at 286 °C. In the second run, endothermic peak 2 appeared at 30 °C. T_g may be assigned to endothermic peak 1 and T_c may be assigned to exothermic peak 2. T_g of sodium alginate was reported to be 158°C. [17,18] and T_g of guar gum was reported to be 108.25 °C [19]. The results are in good agreement with the reported data.

Zeta sizer of SA@GG@IACC Composites (before adsorption) was performed. Water is used as a dispersant media. Dispersant RI and viscosity were 1.330 and 0.8872, respectively. Material RI was found to be 1.59. The temperature was kept at 25 °C. The average Z-size of the composites was found to be 161.9 d.nm. PdI (Polydispersity Index) was found to be 0.062. The intercept was found to be 0.677. Peak 1 appeared at 181.3 d.nm with a standard deviation of 44.26 d.nm. The size distribution by intensity is given below.

Zeta potential of SA@GG@IACC Composites (before adsorption) was performed (Figure 6). Water is used as a dispersant media. Dispersant RI and Viscosity was found to be 1.300 and 0.8872, respectively. The temperature was kept at 25 °C and the number

of zeta runs was 24. Zeta potential was found to be −47.7 mV in water. Zeta potential tells us about the stability behavior of the composites (Figure S1). DB86 is anionic dye, and these dyes have a sulfonate group on their surface in solution form, due to which it gives a negative value of zeta potential at pH 3 [20]. As the zeta potential was found to be −47.7 mV, zeta potential from ±40 to ±60 (mV) exhibits good stability of the composites, and it also shows that flocculation or agglomeration does not occur. Agglomeration only occurs if the zeta potential values are low. The results are in good agreement with the reported data [21–26].



Formula	mass%	Atom%	Sigma	Net	K ratio	Line
C	28.55	37.93	0.03	45683	0.0093238	K
O	50.51	50.38	0.09	127659	0.1190653	K
Al	18.02	10.66	0.05	294912	0.0858374	K
Ca	1.77	0.70	0.02	25876	0.0117143	K
Fe	1.16	0.33	0.02	6864	0.0066023	K
Total	100.00	100.00				

Figure 4. EDX of SA@GG@ICAA Composites (Before Adsorption).

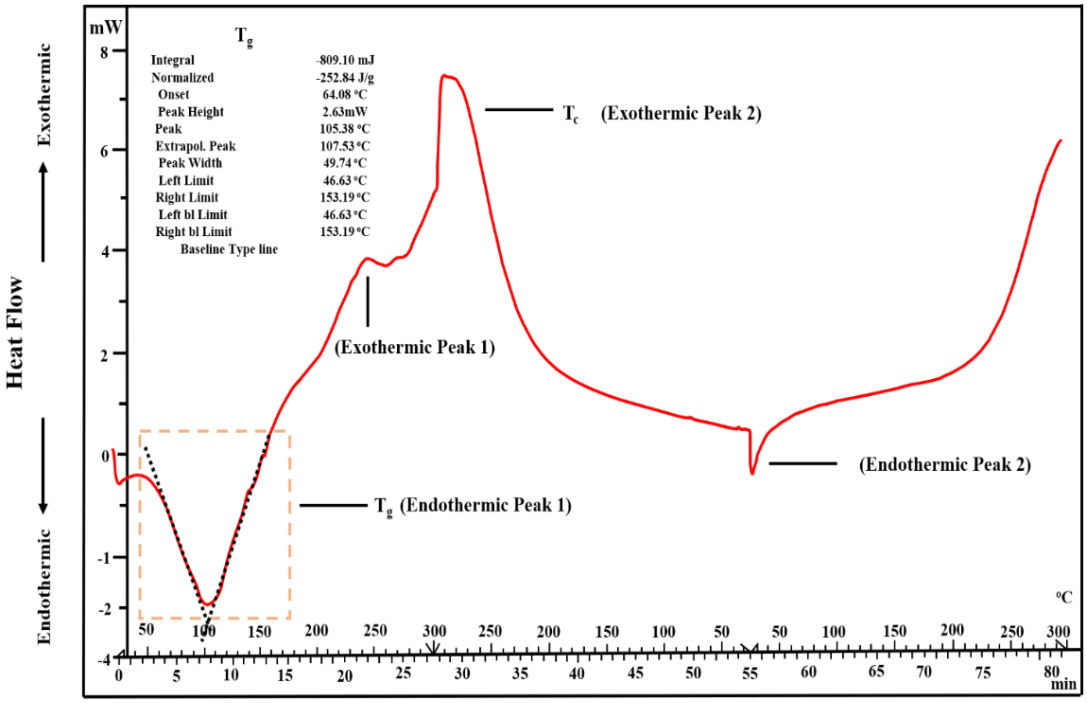


Figure 5. DSC of SA@GG@ICAA Composites (B.A).

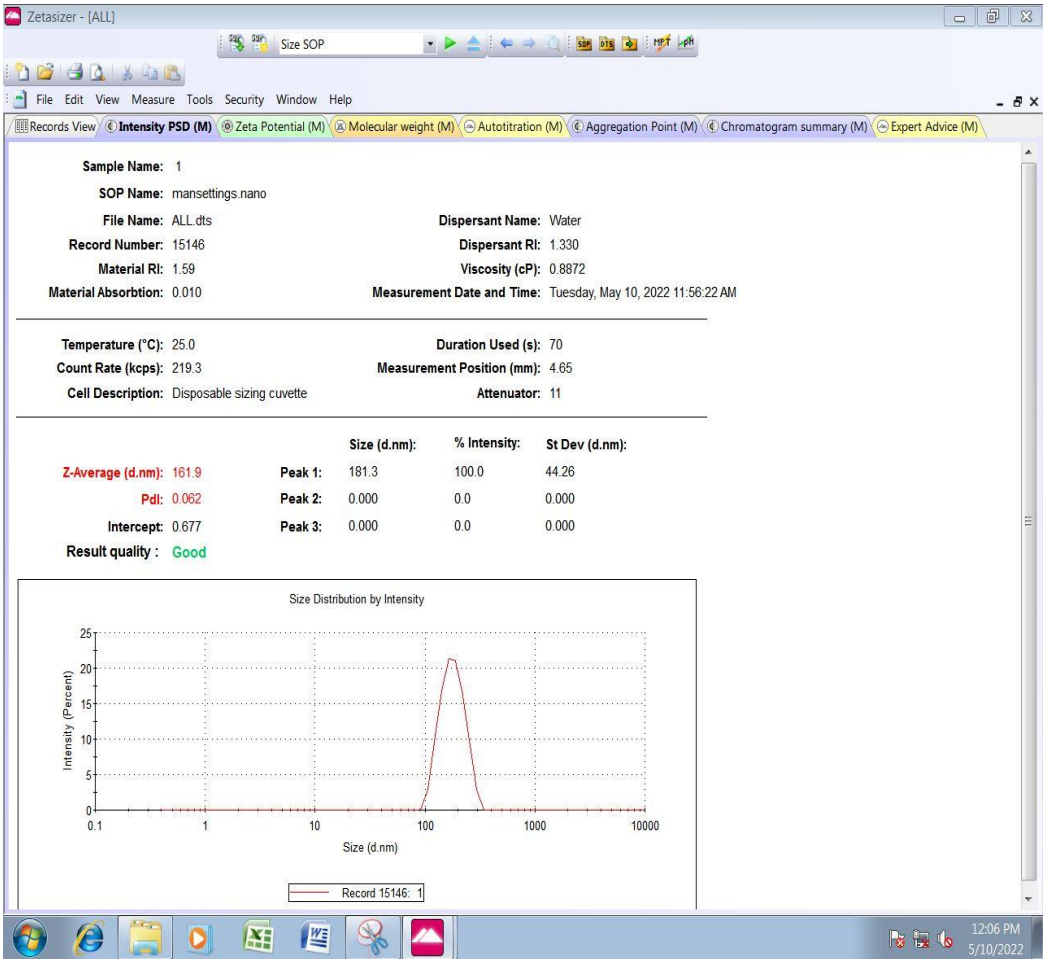


Figure 6. Size Distribution of SA@GG@IACC Composites (Before Adsorption).

BET was performed on pure composites of sodium alginate, guar gum and iron coated activated alumina (before adsorption). The N_2 adsorption–desorption isotherm as given in Figure S2 depicted a Type II isotherm with Hysteresis Loop H4. The surface area was found to be 5.606 m^2/g, pore size, which was determined by the SF Method, was found to be 0.453 nm (4.53 Å) and pore volume was found to be 0.0431 cc/g. Pore size that was determined by HK method was found to be 0.432 nm (4.32 Å) and pore volume was found to be 0.058 cc/g. The results are in good agreement with the reported data (Table S1).

FTIR was performed on the adsorbent to determine the functional groups which are present on the surface of the adsorbent and are involved in the attachment of the adsorbate to the adsorbent surface. The IR spectra show the various peaks which denote different functional groups present in the adsorbent. The range of the IR-spectra is from 400 cm^{-1} to 4000 cm^{-1}; results obtained from the FTIR analysis of the adsorbent are shown in Figure 7.

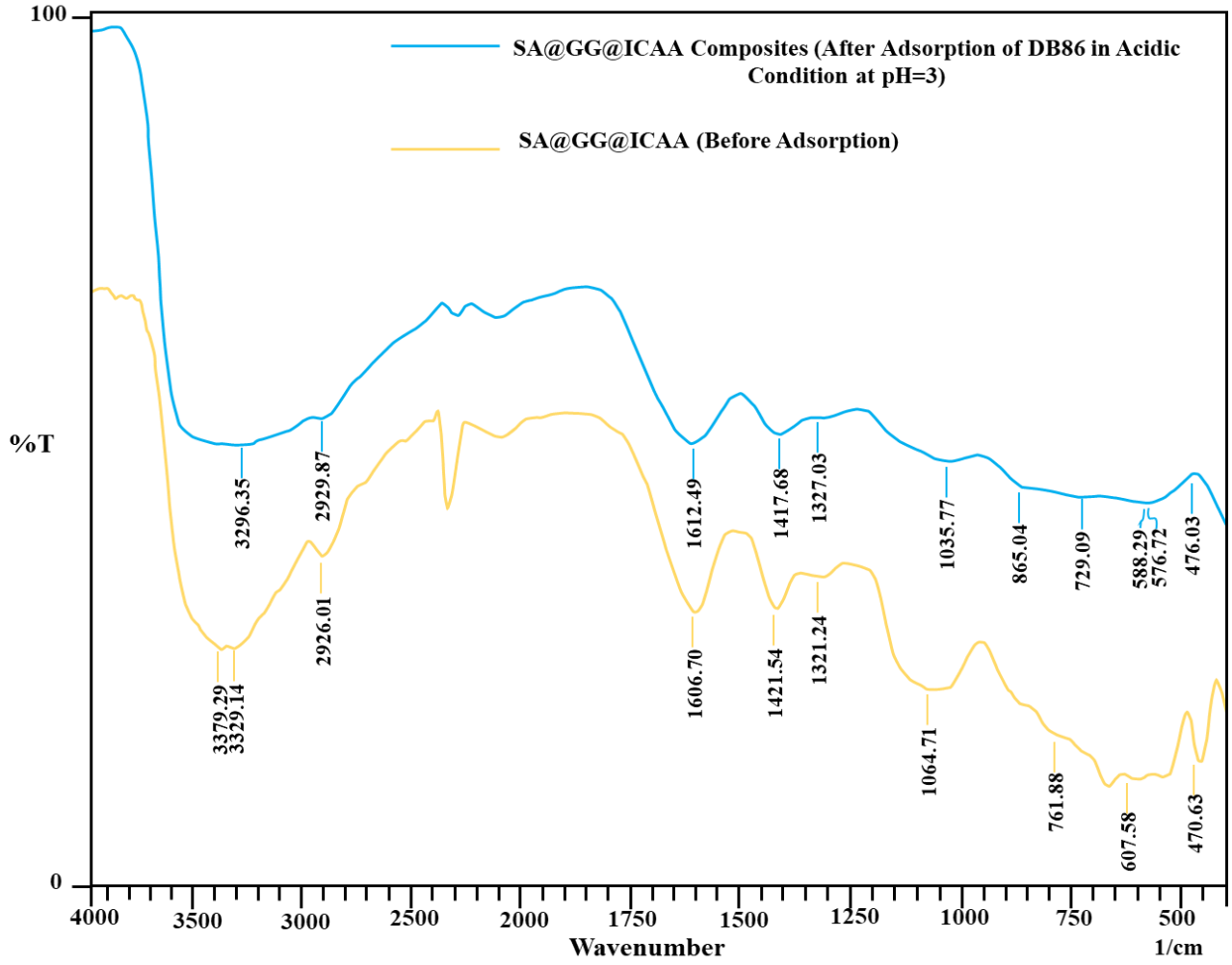


Figure 7. FTIR of SA@GG@ICAA Composites (Before and after adsorption DB86 Dye).

FTIR spectra of SA@GG@ICAA Composites (before and after adsorption of dyes) is given in Figure 7. The appearance of broad and strong peaks at 3379 and 3329 are attributed to the O-H stretching vibration and a slight shift is observed. The strong peaks at 2926 are attributed to the C-H stretching and the strong peak at 1421 is due to the symmetric stretching or asymmetric stretching of carboxylate COO^- vibrations. A prominent peak at 761 appears due to Al–O stretching and at 607 due to Fe-O stretching.

In sodium alginate, guar gum and iron coated activated alumina composites (after adsorption of Direct Blue 86 dye in acidic conditions at pH = 3) the change in position of band from 3379 to 3296 can be attributed to the adsorption of dye on the surface of the

composites. Similarly, a shift in absorption band from 1606 to 1612 and 1061 to 1035 is found after adsorption of dye on the adsorbent surface [27]. The appearance of broad and strong peaks at 1035 indicate C-O-C stretching of the glyosidic linkage or the stretching vibration of the S-O(SO_3-H) group [28–32].

3.2. Paramers Optimization

Different adsorption parameters were optimized, i.e., adsorbate concentration, contact time, pH and adsorbent concentration to obtain best adsorption values for the removal of the selected dye.

There is an increase in adsorption as the concentration of dye increases up to 40 ppm, and then there is no significant increase in adsorption as the concentration rises, as saturation of the adsorbent occurs and all the active sites of the adsorbent are occupied. Thus, there is no significant increase in adsorption after 40 ppm.

The time factor also has a significant effect on adsorption capacity, and maximum adsorption was achieved at 150 min of shaking time. The adsorbent amount has found a positive influence on the removal of dye, and maximum removal was achieved under acidic conditions at pH 3 as shown in Figure 8.

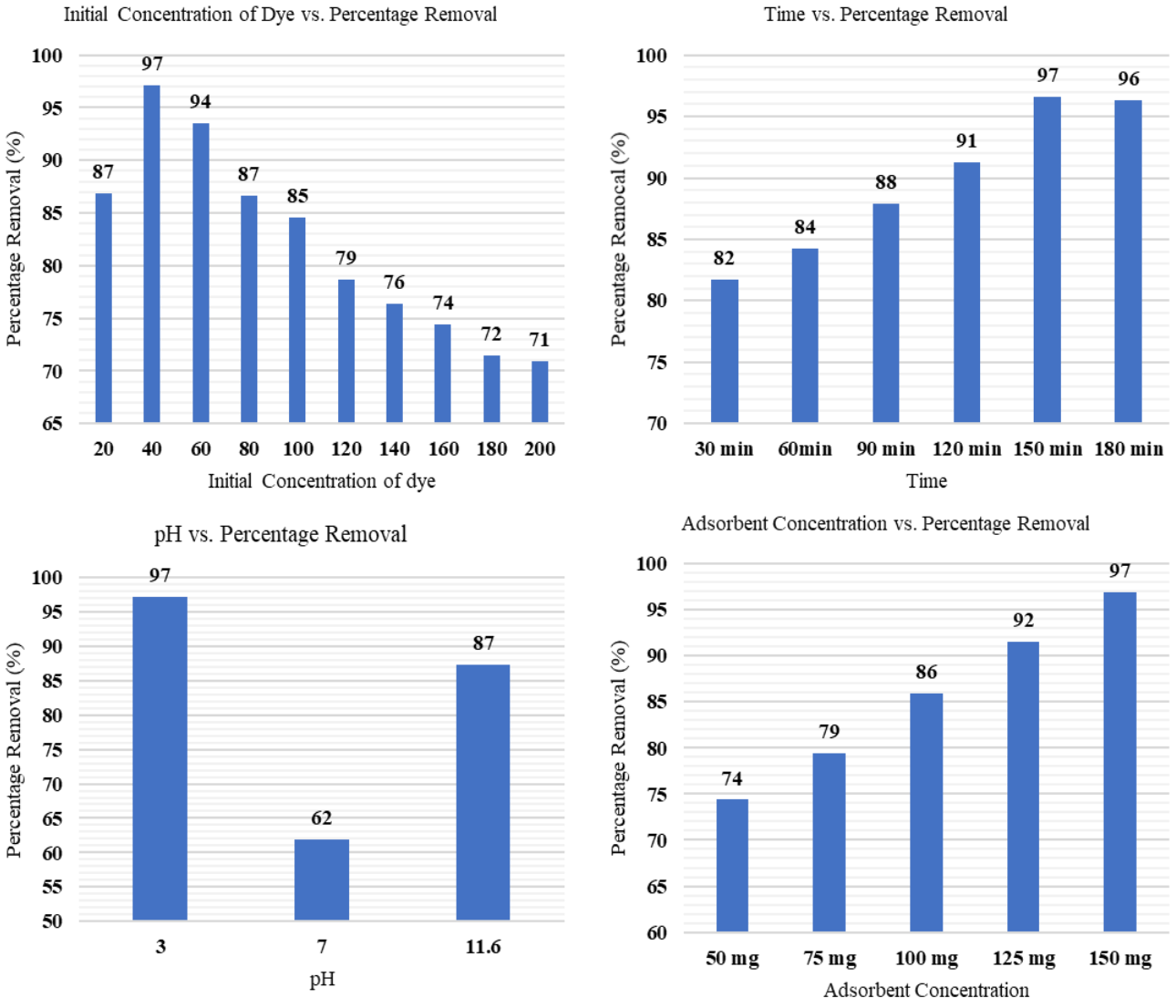


Figure 8. Effect of different adsorption parameters.

3.3. Adsorption Isotherms

The equilibrium relationship between the adsorbate adsorbed on the surface of the adsorbent at constant temperature was studied. Adsorption isotherms are important and were used to know the interaction between the adsorbent and the adsorbate. When designing adsorption systems, the equilibrium adsorption isotherm is crucial. There are various isotherms equations known for solid–liquid systems. The Freundlich isotherm, Langmuir isotherm, Dubinin–Radushkevich (R–D) isotherm, Elovich isotherm and Temkin isotherm are applied in both linear and non-linear forms [33,34]. These isotherms are applied to DB86 dye removal from aqueous media through synthetic composites.

The Freundlich isotherm is based on multilayer adsorption which occurs on heterogeneous surfaces. Studies using the Freundlich isotherm demonstrate that the adsorption occurs on a heterogeneous surface and that its energy is not uniform. Equation (1) is used for the calculation of different parameters of the isotherm.

$$\text{LogCad} = \text{LogK}_F + \frac{1}{n}\text{logC}_e \quad \text{Linear Form} \tag{1}$$

$$C_{ad} = K_F C_e^{1/n} \qquad \text{Non-linear Form} \tag{2}$$

C_{ad} is the amount of specie adsorbed
C_e is remaining concentration in solution after adsorption
K_F = relative adsorption capacity
1/n = adsorption intensity [35].

The adsorption phenomenon is considered promising if K_F values ranges from 1 to 20. Results indicate K_F is 8.76 for the adsorption of DB86.

For DB86, the non-linear Freundlich isotherm was found to be best fitted compared to its linear form, as R^2 was found to be 0.942 for the non-linear form. 1/n for the linear form was found to be 0.422237 and for the non-linear form was 0.412, which indicates a normal Freundlich adsorption process (Figure 9).

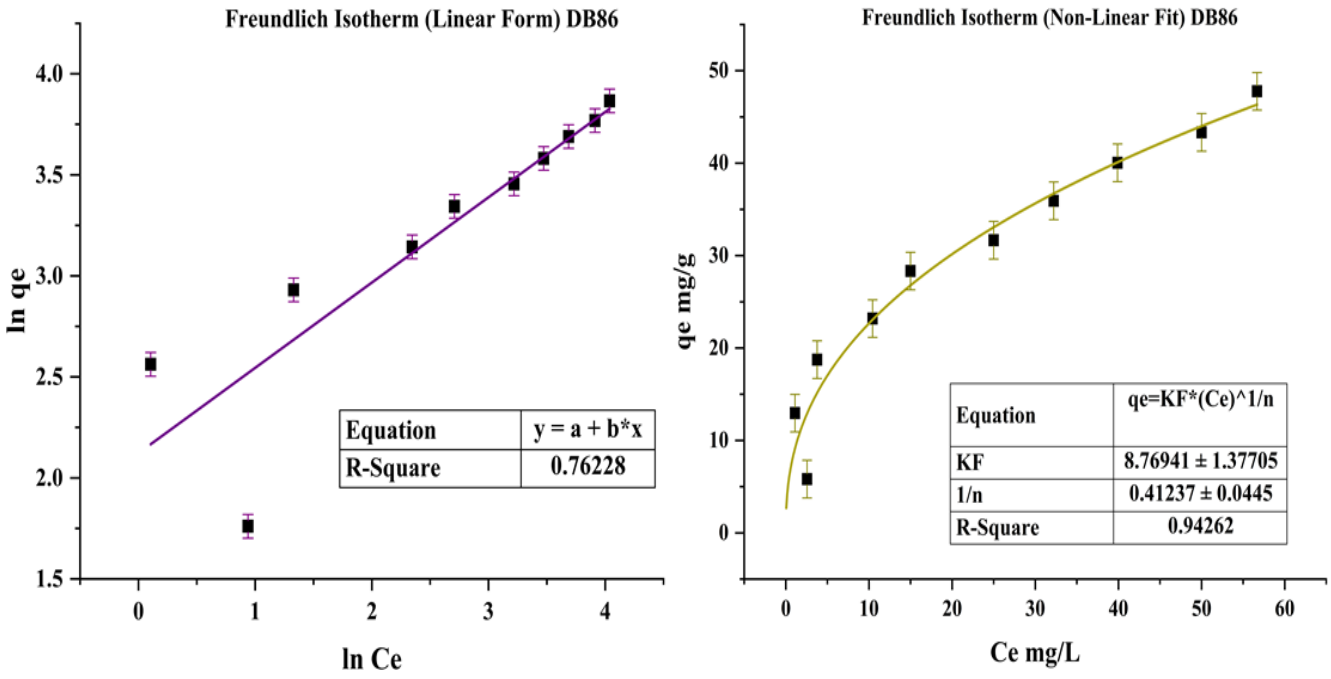


Figure 9. Linear and Non-Linear forms of Freundlich Isotherm.

There is no lateral interaction between the adsorbed molecules, according to the Langmuir isotherm, which is based on the monolayer coverage prediction of the adsorbate.

It is assumed that there is no lateral contact between the adsorbed molecules and that the adsorption occurs at particular homogenous sites within the adsorbent. The Langmuir model implies uniform energies for adsorption onto the surface and a lack of adsorbate transmigration on the plane of the surface (Figure 10).

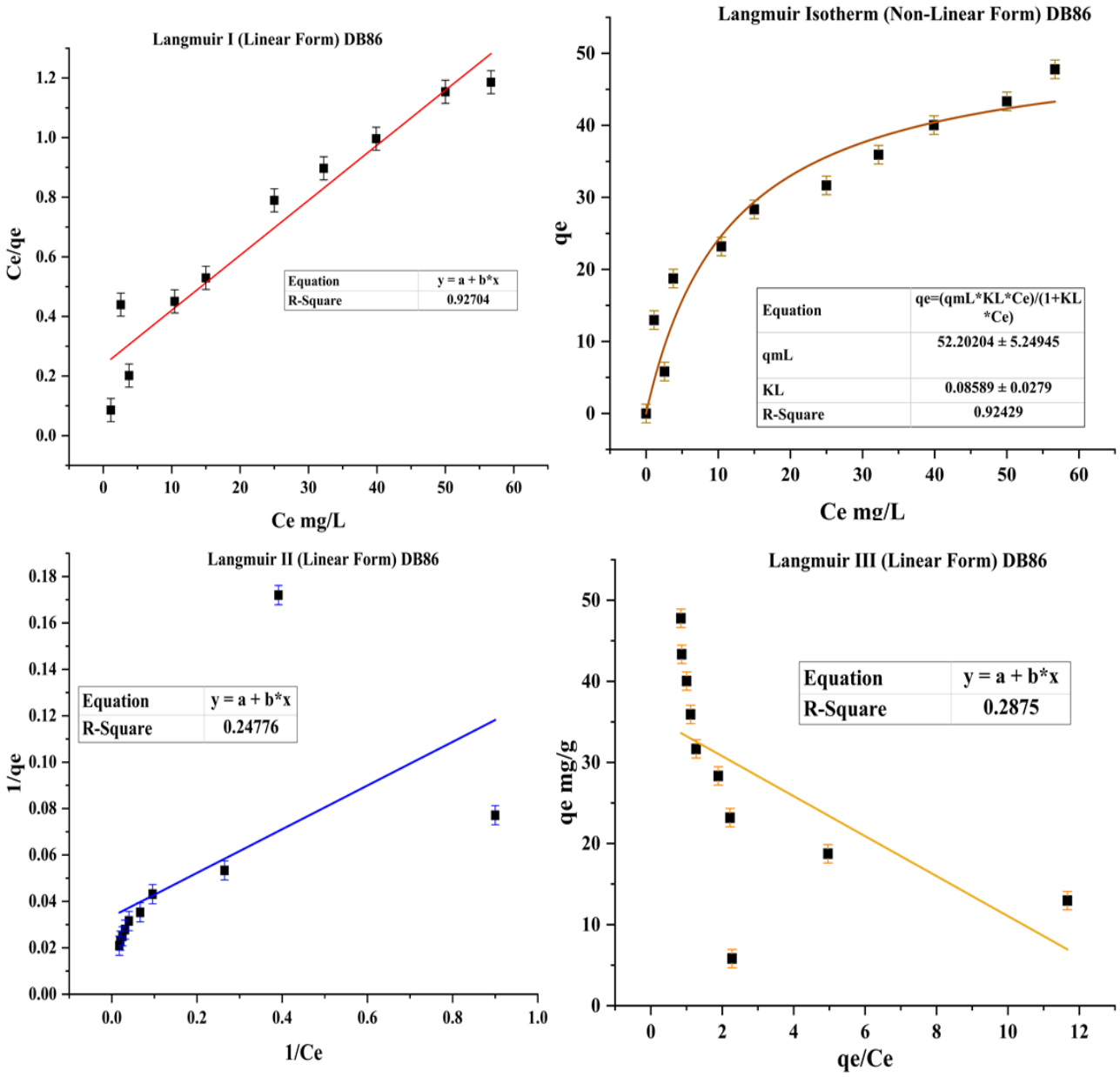


Figure 10. Langmuir Isotherm, Linear and Non-Linear forms of Type I and II.

R_L is another characteristic of the Langmuir isotherm which determines the nature of adsorption and it is given by the following equation; R_L values vary from 0–1 [36–40].

$$R_L = \frac{1}{1 + K_L C_o} \tag{3}$$

For DB86, both the linear and non-linear forms of Langmuir 1 were found to be best fitted as the R^2 values were found to be 0.927 and 0.924 for linear and non-linear forms, respectively. Langmuir II, III and IV do not give good results as the values of R^2 were found to be 0.247, 0.287 and 0.287, respectively.

Due to its complexity, the Dubinin-Radushkevich model is less employed to liquid phase adsorption. It will accept surfaces that have a Gaussian energy distribution. It distinguishes a crucial metric, particularly mean free energy, which is used to separate between physical and chemical adsorption as given in Figure 11.

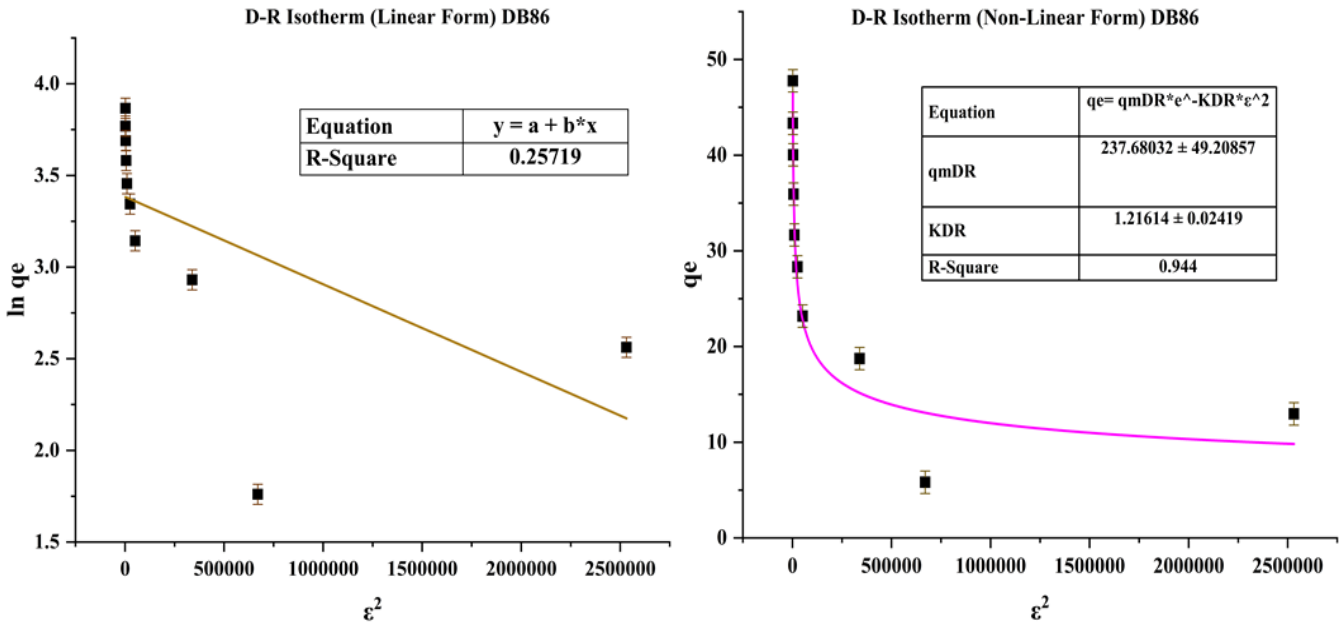


Figure 11. Dubinin-Radushkevich Isotherm.

For DB86, the non-linear form of the D-R Isotherm fitted best as its R^2 value was found to be 0.94, compared to the linear form whose R^2 value was found to be 0.257.

The Elovich isotherm implies a multilayer adsorption because it states that the number of adsorption sites increases exponentially with adsorption (Figure 12).

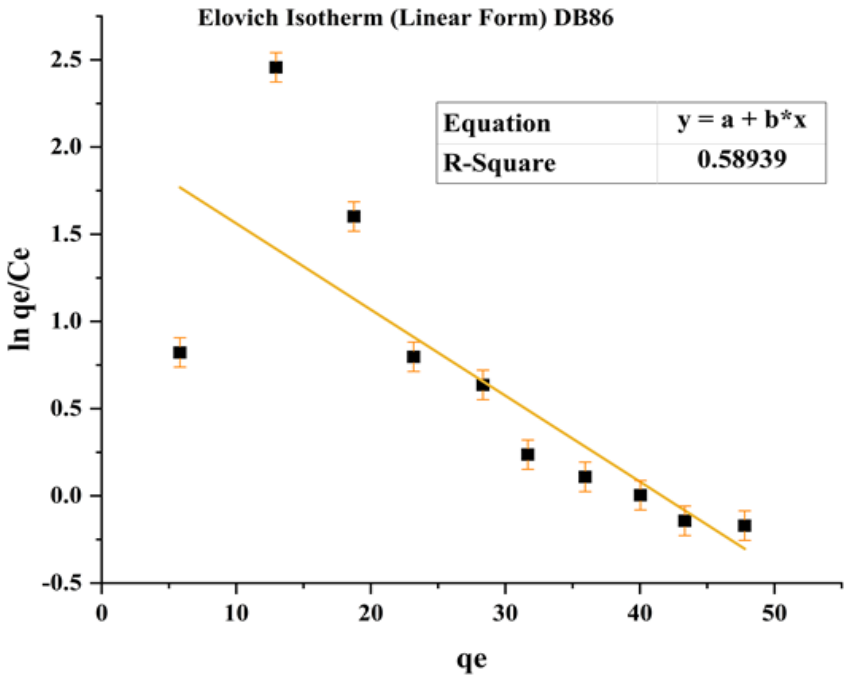


Figure 12. Elovich Isotherm for DB86.

For DB86, the linear form of the Elovich Isotherm is slightly good for the dye as the R^2 value was found to be 0.589.

The Temkin isotherm equation makes two assumptions: first, that the heat of adsorption of all the molecules in the layer decreases linearly with treatment as a result of adsorption phenomenon, and second, that the adsorption is characterized by a uniform distribution of the binding energies up to a maximum binding energy.

For DB86, both linear and non-linear forms of Temkin Isotherm fitted best with the dye as their R^2 values were found to be 0.88 and 0.92, respectively. However, the non-linear form comparatively fitted better than the non-linear form. Both forms are given in Figure 13.

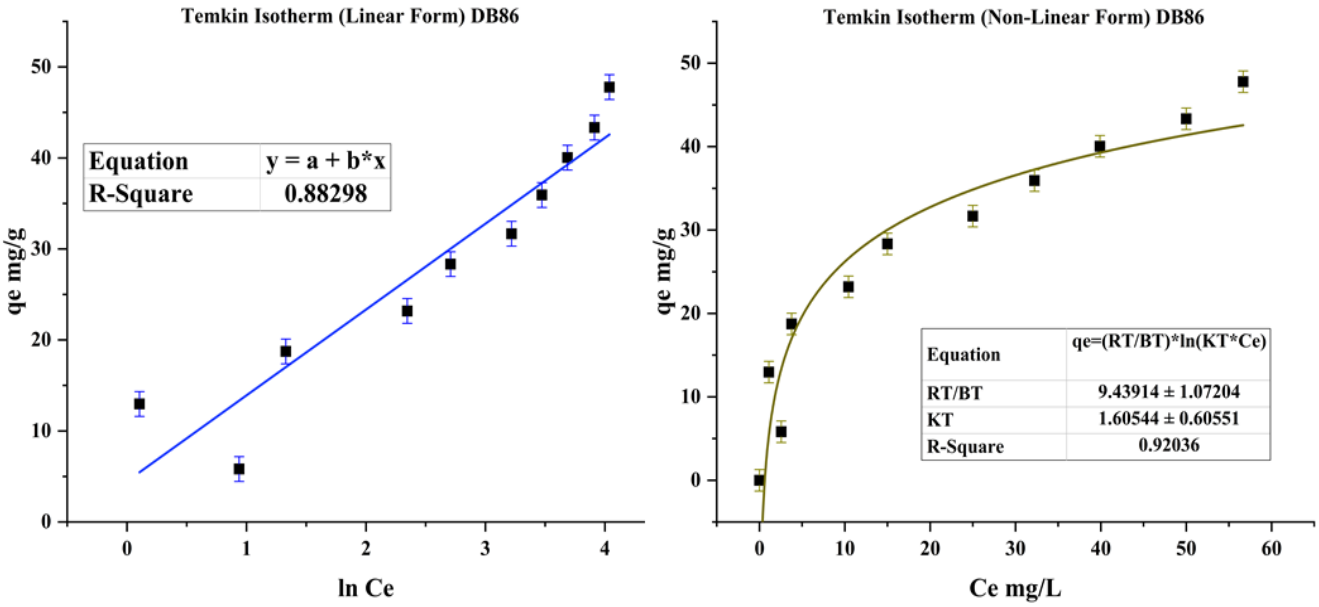


Figure 13. Linear and Non-Linear form of Temkin Isotherm.

3.4. Kinetic Study

Adsorption kinetics are essential for illustrating the rate of adsorbate uptake and the amount of time required for adsorption. This research involved conducting a kinetic investigation for the adsorption of DB86 at various intervals of time. Pseudo-first order and pseudo-second order kinetic models were used to study the adsorption process (Figure 14). The findings of this experiment demonstrate that as the time interval increases, so does the amount of dye adsorbed on the sorbent. Although there was a significant rise at the beginning of the experiment, a decrease in dye adsorption was seen with time. This can be explained by the fact that the adsorbent has a large number of active sites available at the beginning of the process.

Lower solute concentrations are more suited for the pseudo-first order kinetic model. The following equation represents the pseudo-first order kinetic model:

$$\frac{dq_t}{d_t} = K_1(q_e - q_t) \tag{4}$$

For DB86, the non-linear form of PFO fitted best as its R^2 value was found to be 0.983, compared to its linear form whose R^2 value was found to be 0.586.

The following rate equation can be used to calculate the pseudo-second order kinetics:

$$\frac{dq_t}{d_t} = K_2(q_e - q_t)^2 \tag{5}$$

$$K_2 = \text{pseudo-second order rate constant (g/mg·min)} \tag{6}$$

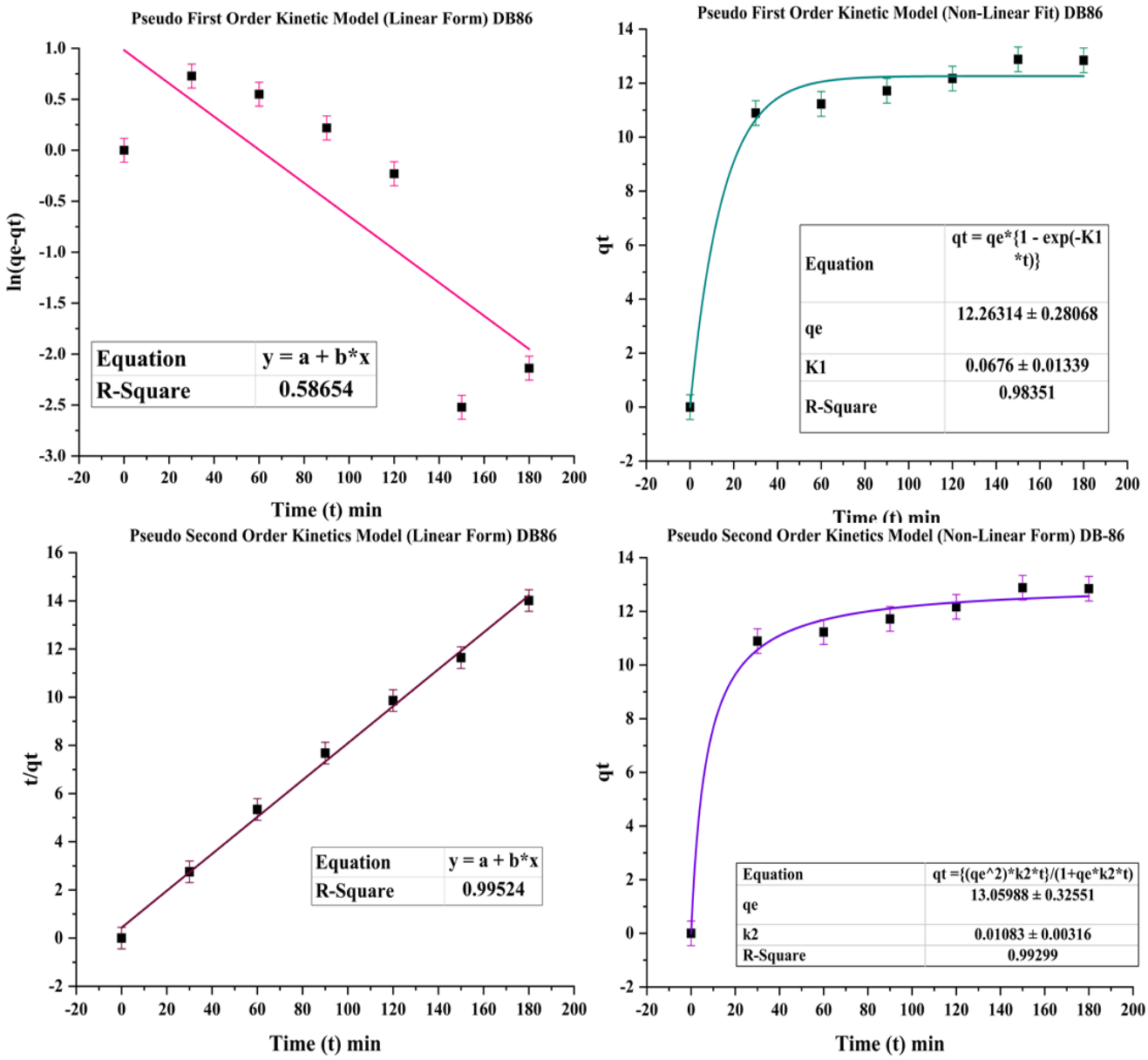


Figure 14. Pseudo-first and -Second Order Kinetics applied on DB86 Adsorption.

With initial conditions of $t = 0$ and $qt = 0$, the equation given above provides a linear equation on integration.

$$\frac{t}{q_t} = \frac{1}{K_2 q_e^2} + \frac{t}{q_e} \tag{7}$$

Initial sorption rate, denoted by h (mg/g·min) corresponds to the term $K_2 q_e^2$ and the non-linear form is expressed as follows:

$$q_t = \frac{q_e^2 K_2 t}{1 + q_e K_2 t} \tag{8}$$

The graphical representation of the pseudo-second order kinetic model is shown by a linear plot of t/q_t vs. t. On the basis of error function, we select the best fitted kinetic equation. Linear regression is usually used to identify the best-fitting kinetic model. The equilibrium adsorption amount qe of the pseudo-first order and pseudo-second order were calculated using the slopes and intercepts of plots of the linear representations [36–40].

For DB86, both linear and non-linear forms of PSO fitted best for the dye as their R^2 values were found to be 0.995 and 0.992, respectively.

3.5. Adsorption Mechanism

Adsorption of DB86 was found at maximum in an acidic pH range. This may be due to hydrogen ions (H^+) which make the surface of the adsorbent positive in an acidic range, and the anionic dye makes a strong electrostatic attraction with the adsorbent (Figure 15). On the other hand, in a basic pH range, the surface of the adsorbent is negatively charged so not suitable for the attachment of the dye. The adsorption mechanism of the dye may be electrostatic attraction between a positively charged adsorbent surface and a negatively charged dye [7].

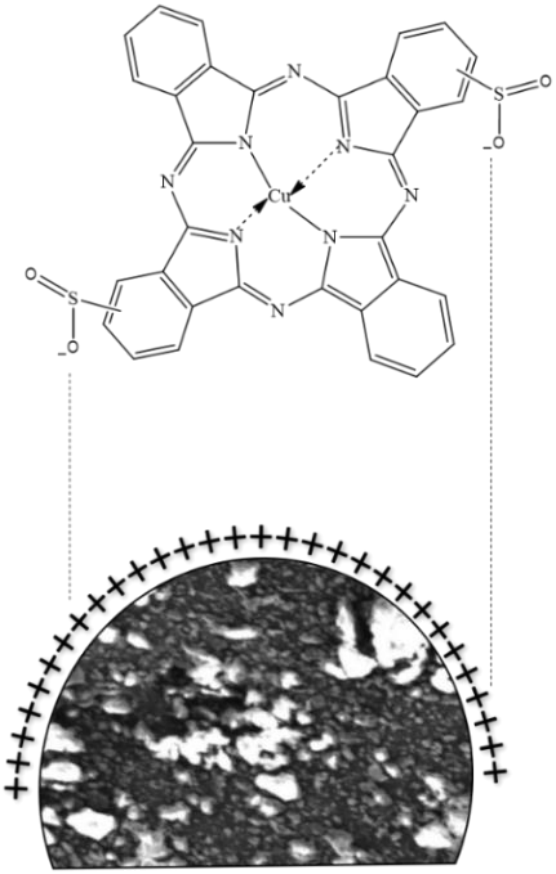


Figure 15. Adsorption of DB86 onto SA@GG@ICAA Composites.

3.6. Regeneration of Composites

Synthetic composites were regenerated by treating with 0.1 M HCI solution for 3 h with constant shaking. After filtration, it was washed three times with distilled water to completely remove acidic components before use for the next adsorption step.

4. Conclusions

The textile industry is one of the biggest industries of Pakistan. Unfortunately, in developing countries waste water of these industries is directly discharged into environment without any treatment due to the high cost of treatment plants. These dyes are also a major cause of numerous diseases, such as cancer. This study aims to remove harmful dyes from water bodies by employing a cost-effective material. For the removal these harmful dyes, a novel adsorbent is developed which was synthesized by using sodium alginate, guar gum and iron coated activated alumina (SA@GG@ICAA Composites) with the Ion Gelation

Method. The novel composites were characterized by using SEM, XRD, DSC, FTIR, BET, EDX, zeta potential and zeta sizer. Characterization provides information about amorphous nature of the composites with different functional groups available on the surface for attachment of dye. The batch adsorption experiment shows 97% removal efficiency of DB86 by employing the composites. Kinetic and isothermal studies give information about the physical nature of adsorption with electrostatic attraction. Synthesized composites are found to be quite competent for quick removal of DB86 dye from aqueous media.

Supplementary Materials: The following supporting information can be downloaded at: https://www.mdpi.com/article/10.3390/coatings13010103/s1, Figure S1: Zeta Potential of SA@GG@IACC Composites (B.A); Figure S2. N_2 Adsorption–Desorption Isotherm; Figure S3. HK-SF Pore Size Distribution; Figure S4. Plot P/Po Vs. 1/[W{(Po/P)-1].

Author Contributions: Conceptualization, F.B. and A.I.; methodology, F.B. and S.K.; software, F.B. and G.S.; validation, A.M., S.K. and G.S.; formal analysis, S.A.A.-H. and S.K.; investigation, A.M. and S.A.A.-H.; resources, S.A.A.-H.; data curation, F.B. and A.I.; writing—original draft preparation, F.B. and S.K.; writing—review and editing, F.B., A.I. and M.E.A.Z.; visualization, A.M. and S.A.A.-H.; supervision, F.B.; project administration, M.E.A.Z.; funding acquisition, S.A.A.-H., A.I. and M.E.A.Z. All authors have read and agreed to the published version of the manuscript.

Funding: The authors extend their appreciation to the Deanship of Scientific Research at Imam Mohammad Ibn Saud Islamic University for funding this work through Research Group no. RG 21-09-77.

Institutional Review Board Statement: Not applicable.

Informed Consent Statement: Not applicable.

Data Availability Statement: Data is available in the manuscript and Supplementary Material.

Acknowledgments: Authors acknowledge the technical support provided by Hi-Tech lab, University of Sargodha, regarding analysis of the samples for heavy metals reported in this study.

Conflicts of Interest: The authors declare no conflict of interest.

References

1. Krishnappa, B.; Bhat, V.S.; Ancy, V.; Joshi, J.C.; Naik, M.; Hegde, G.J.M. Biowaste-Derived, Highly Efficient, Reusable Carbon Nanospheres for Speedy Removal of Organic Dyes from Aqueous Solutions. *Molecules* **2022**, *27*, 7017. [CrossRef] [PubMed]
2. Tilt, B.J.H.O. Perceptions of risk from industrial pollution in China: A comparison of occupational groups. *Human Organ.* **2006**, *65*, 115–127. [CrossRef]
3. Owa, F.D. Water pollution: Sources, effects, control and management. *Mediterr. J. Soc. Sci.* **2013**, *4*, 65. [CrossRef]
4. Weiner, E.R. *Applications of Environmental Chemistry: A Practical Guide for Environmental Professionals*; CRC Press: Boca Raton, FL, USA, 2010.
5. Khan, S.; Malik, A. Environmental and health effects of textile industry wastewater. In *Environmental Deterioration and Human Health*; Springer: Berlin/Heidelberg, Germany, 2014; pp. 55–71.
6. Kant, R. Textile dyeing industry an environmental hazard. *J. Nat. Sci.* **2012**, *4*, 22–26. [CrossRef]
7. El Nemr, A.; Abdelwahab, O.; El-Sikaily, A.; Khaled, A. Removal of direct blue-86 from aqueous solution by new activated carbon developed from orange peel. *J. Hazard. Mater.* **2009**, *161*, 102–110. [CrossRef]
8. Gita, S.; Hussan, A.; Choudhury, T.J.E.E. Impact of textile dyes waste on aquatic environments and its treatment. *Environ. Ecol.* **2017**, *35*, 2349–2353.
9. Padma, G.T.; Rao, T.S.; Naidu, K.C.B. Preparation, characterization and dielectric properties of sodium alginate/titanium dioxide composite membranes. *SN Appl. Sci.* **2018**, *1*, 75. [CrossRef]
10. Verma, A.; Thakur, S.; Mamba, G.; Gupta, R.K.; Thakur, P.; Thakur, V.K. Graphite modified sodium alginate hydrogel composite for efficient removal of malachite green dye. *Int. J. Biol. Macromol.* **2020**, *148*, 1130–1139. [CrossRef]
11. Zhao, X.; Wang, X.; Lou, T. Preparation of fibrous chitosan/sodium alginate composite foams for the adsorption of cationic and anionic dyes. *J. Hazard. Mater.* **2021**, *403*, 124054. [CrossRef]
12. Racoviţă, S.; Vasiliu, S.; Popa, M.; Luca, C. Polysaccharides based on micro-and nanoparticles obtained by ionic gelation and their applications as drug delivery systems. *Rev. Roum. De Chim.* **2009**, *54*, 709–718.
13. Shahid, M.; Bukhari, S.A.; Gul, Y.; Munir, H.; Anjum, F.; Zuber, M.; Jamil, T.; Zia, K.M. Graft polymerization of guar gum with acryl amide irradiated by microwaves for colonic drug delivery. *Int. J. Biol. Macromol.* **2013**, *62*, 172–179. [CrossRef]

14. Zhong, Z.Y.; Prozorov, T.; Felner, I.; Gedanken, A. Sonochemical Synthesis and Characterization of Iron Oxide Coated on Submicrospherical Alumina: A Direct Observation of Interaction between Iron Oxide and Alumina. *J. Phys. Chem. B* **1999**, *103*, 947–956. [CrossRef]
15. Kim, S.-G.; Lim, G.-T.; Jegal, J.; Lee, K.-H. Pervaporation separation of MTBE (methyl tert-butyl ether) and methanol mixtures through polyion complex composite membranes consisting of sodium alginate/chitosan. *J. Membr. Sci.* **2000**, *174*, 1–15. [CrossRef]
16. Ionita, M.; Pandele, M.A.; Iovu, H. Sodium alginate/graphene oxide composite films with enhanced thermal and mechanical properties. *Carbohydr. Polym.* **2013**, *94*, 339–344. [CrossRef]
17. Roger, S.; Bee, A.; Balnois, E.; Bourmaud, A.; Le Deit, H.; Grohens, Y. Physical and Mechanical Properties of Alginate Films Containing Calcium Cations and Ferrofluids. In Proceedings of the 5th International Conference on Polymer-Solvent Complexes & Intercalates, Lorient, France, 11–13 July 2004.
18. Shaari, N.; Kamarudin, S.J.P.T. Sodium alginate/alumina composite biomembrane preparation and performance in DMFC application. *Polym. Test.* **2020**, *81*, 106183. [CrossRef]
19. Kumar, A.; De, A.; Mozumdar, S. Synthesis of acrylate guar-gum for delivery of bio-active molecules. *Bull. Mater. Sci.* **2015**, *38*, 1025–1032. [CrossRef]
20. Kuo, C.-Y.; Wu, C.-H.; Wu, J.-Y. Adsorption of direct dyes from aqueous solutions by carbon nanotubes: Determination of equilibrium, kinetics and thermodynamics parameters. *J. Colloid Interface Sci.* **2008**, *327*, 308–315. [CrossRef]
21. Parveen, S.; Rana, S.; Fangueiro, R. A review on nanomaterial dispersion, microstructure, and mechanical properties of carbon nanotube and nanofiber reinforced cementitious composites. *J. Nanomater.* **2013**, *2013*, 1–19. [CrossRef]
22. Alsharef, J.M.; Taha, M.R.; Khan, T.A. Physical dispersion of nanocarbons in compositesâ€"a review. *J. Teknol.* **2017**, *79*, 5. [CrossRef]
23. Caon, T.; Zanetti-Ramos, B.G.; Lemos-Senna, E.; Cloutet, E.; Cramail, H.; Borsali, R.; Soldi, V.; Simoes, C.M.O. Evaluation of DNA damage and cytotoxicity of polyurethane-based nano-and microparticles as promising biomaterials for drug delivery systems. *J. Nanoparticle Res.* **2010**, *12*, 1655–1665. [CrossRef]
24. Bhargava, S.; Chu, J.J.H.; Valiyaveettil, S. Controlled Dye Aggregation in Sodium Dodecylsulfate-Stabilized Poly(methylmethacrylate) Nanoparticles as Fluorescent Imaging Probes. *ACS Omega* **2018**, *3*, 7663–7672. [CrossRef] [PubMed]
25. Mahajan, A.; Ramana, E.V. Patents on magnetoelectric multiferroics and their processing by electrophoretic deposition. In *Recent Patents on Materials Science*; Bentham Science Publishers: Sherga, United Arab Emirates, 2014; Volume 7, pp. 109–130.
26. Clogston, J.D.; Patri, A.K. *Zeta Potential Measurement. Characterization of Nanoparticles Intended for Drug Delivery*; Springer: Berlin/Heidelberg, Germany, 2011; pp. 63–70.
27. Garg, D.; Majumder, C.; Kumar, S.; Sarkar, B.J. Removal of Direct Blue-86 dye from aqueous solution using alginate encapsulated activated carbon (PnsAC-alginate) prepared from waste peanut shell. *J. Environ. Chem. Eng.* **2019**, *7*, 103365. [CrossRef]
28. Topuz, B.B.; Gündüz, G.; Mavis, B.; Çolak, Ü.J.D. Pigments, Synthesis and characterization of copper phthalocyanine and tetracarboxamide copper phthalocyanine deposited mica-titania pigments. *Dye. Pigment.* **2013**, *96*, 31–37. [CrossRef]
29. Magisetty, R.; Prajapati, D.; Ambekar, R.; Shukla, A.; Kandasubramanian, B. β-Phase Cu-phthalocyanine/acrylonitrile butadiene styrene terpolymer nanocomposite film technology for organoelectronic applications. *J. Phys. Chem. C* **2019**, *123*, 28081–28092. [CrossRef]
30. Athanasiu, A.A.; Deaconu, M.; Crudu, M.; Doncea, S.; Stoica, R.; Oproiu, L.; Senin, R.; Ruse, M.; Rosu, D.; Filipescu, C. Synthesis and Characterization of Nanosized Copper (II)-Phthalocyanine Pigment (P BI 15: 3) with the Modified Surface. I. *Rev. De Chim.* **2017**, *68*, 343–349. [CrossRef]
31. Nauka, K.; Zhao, Y.; Ng, H.-T.; Hanson, E.G. Surface Molecular Vibrations as a Tool for Analyzing Surface Impurities in Copper Phthalocyanine Organic Nanocrystals. *MRS Proc.* **2010**, *1270*, 659. [CrossRef]
32. Eshkalak, S.K.; Khatibzadeh, M.; Kowsari, E.; Chinnappan, A.; Ramakrishna, S. Pigments, A novel surface modification of copper (II) phthalocyanine with ionic liquids as electronic ink. *Dye. Pigment.* **2018**, *154*, 296–302. [CrossRef]
33. Mourabet, M.; El Boujaady, H.; El Rhilassi, A.; Ramdane, H.; Bennani-Ziatni, M.; El Hamri, R.; Taitai, A. Defluoridation of water using Brushite: Equilibrium, kinetic and thermodynamic studies. *Desalination* **2011**, *278*, 1–9. [CrossRef]
34. Priyantha, N.; Lim, L.; Dahri, M.K.; Tennakoon, D.T.B. Dragon Fruit Skin as a Potential Low-Cost Biosorbent for the Removal of Manganese(II) Ions. *J. Appl. Sci. Environ. Sanit.* **2013**, *8*, 179–188.
35. Dada, A.O.; Olalekan, A.P.; Olatunya, A.M.; Dada, O. Langmuir, Freundlich, Temkin and Dubinin–Radushkevich isotherms studies of equilibrium sorption of Zn^{2+} unto phosphoric acid modified rice husk. *IOSR J. Appl. Chem.* **2012**, *3*, 38–45.
36. López-Luna, J.; Ramírez-Montes, L.E.; Martinez-Vargas, S.; Martínez, A.I.; Mijangos-Ricardez, O.F.; González-Chávez, M.d.C.A.; Carrillo-González, R.; Solís-Domínguez, F.A.; Cuevas-Díaz, M.d.C.; Vázquez-Hipólito, V. Linear and nonlinear kinetic and isotherm adsorption models for arsenic removal by manganese ferrite nanoparticles. *Appl. Sci.* **2019**, *1*, 950. [CrossRef]
37. Karthik, V.; Selvakumar, P.; Sivarajasekar, N.; Megavarshini, P.; Brinda, N.; Kiruthika, J.; Balasubramani, K.; Ahamad, T.; Naushad, M. Comparative and Equilibrium Studies on Anionic and Cationic Dyes Removal by Nano-Alumina-Doped Catechol Formaldehyde Composite. *J. Chem.* **2020**, *2020*, 7617989. [CrossRef]
38. Benmessaoud, A.; Nibou, D.; Mekatel, E.H.; Amokrane, S.; Engineering, C. A comparative study of the linear and non-linear methods for determination of the optimum equilibrium isotherm for adsorption of Pb2+ ions onto Algerian treated clay. *Iran. J. Chem. Chem.* **2020**, *39*, 153–171.

39. Al-Ma'abreh, A.M.; Abuassaf, R.A.; Hmedat, D.A.; Alkhabbas, M.; Edris, G.; Hussein-Al-Ali, S.H.; Alawaideh, S. Adsorption Characteristics of Hair Dyes Removal from Aqueous Solution onto Oak Cupules Powder Coated with ZnO. *Int. J. Mol. Sci.* **2022**, *23*, 11959. [CrossRef]
40. Ghaffari, H.R.; Pasalari, H.; Tajvar, A.; Dindarloo, K.; Goudarzi, B.; Alipour, V.; Ghanbarneajd, A. Linear and nonlinear two-parameter adsorption isotherm modeling: A case-study. *Int. J. Eng. Sci.* **2017**, *6*, 1–11.

Disclaimer/Publisher's Note: The statements, opinions and data contained in all publications are solely those of the individual author(s) and contributor(s) and not of MDPI and/or the editor(s). MDPI and/or the editor(s) disclaim responsibility for any injury to people or property resulting from any ideas, methods, instructions or products referred to in the content.